Molecular Dynamics Study of Peptide in Water at Different Temperature

U. Chaudhary and G. C. Kaphle

Journal of Nepal Physical Society

Volume 9, Issue 1, June 2023

ISSN: 2392-473X (Print), 2738-9537 (Online)

JNPS, **9** (1): 83-91 (2023)

DOI: https://doi.org/10.3126/jnphyssoc.v9i1.57601

Published by:

Nepal Physical Society
P.O. Box: 2934
Tri-Chandra Campus
Kathmandu, Nepal
Email: nps.editor@gmail.com

JNPS 9 (1): 83-91 (2023)
ISSN: 2392-473X (Print), 2738-9537 (Online)

DOI: https://doi.org/10.3126/jnphyssoc.v9i1.57601

Molecular Dynamics Study of Peptide in Water at Different Temperature

U. Chaudhary and G. C. Kaphle*
Central Department of Physics, Tribhuvan University, Kathmandu, Nepal
*Corresponding Email: gck223@gmail.com, gopi.kaphle@cdp.tu.edu.np

Received: *9th March, 2023;* ***Revised:*** *26th June, 2023;* ***Accepted:*** *29th June, 2023*

ABSTRACT

Molecular dynamics approach has been carried out to study the structural properties of peptide to estimate the self-diffusion coefficients of water at different temperatures 290 K, 300 K, and 310 K respectively. The energy profiles show the stability of system which ensures a well-balanced molecular structure of the system. The radial distribution functions (RDFs) of the solvent-solvent, solute-solute, and solute-solvent show the distribution of system within the required references. The self-diffusion coefficients of water have been determined using respective mean square displacement (MSD) curves through the Einstein's relation. The self-diffusion coefficients of water at different temperatures are 0.44×10^{-5} cm^2s^{-1}, 0.48×10^{-5} cm^2s^{-1}, and 0.50×10^{-5} cm^2s^{-1} respectively. Calculations show that the MSD of water throughout the system is increasing on increasing temperature. The results are also valid with the theoretical as well as available experimental data.

Keywords: Molecular dynamics, Peptide, Radial distribution, Self-diffusion.

INTRODUCTION

Inorganic ions, water, and organic molecules are the main components of majority of a cell. Among them water is the most prevalent molecule. The tightly packed biomolecules in a cell can only interact with one another through direct physical contact [1]. Interactions between water and other cell components are essential to a variety of biological processes in living things. Peptide bonds are the short, sequential chains of amino acids that make up peptides. Most of the meals, including as meat, fish, beans, wheat, flaxseed, hempseed etc. contain peptides [2]. Peptide bonds, in general are produced at the molecular level during dehydration synthesis or reaction processes. It occurs most frequently between amino acids, referred as a condensation reaction. There are 20 common amino acids that occur in the structure of protein and peptide molecules [3]. The amino or NH_2 of one amino acid links to the carboxyl (acid) or COOH group of another amino acid to produce peptide bonds that unite amino acids to make polypeptides and proteins. Amino acids are also called the building blocks of proteins. Proteins typically include 50 to 1000 amino acid residues in each polypeptide chain, and those polypeptides with up to 100 amino acids are referred to as tiny proteins [4]. The motion of smaller molecules such as amino acids and small proteins are hindered by the macromolecular crowding inside cells [5]. To know the overall behavior of such peptides are quite cumbersome. Here, we focus our attentions to find out the behavior of general and anomalous diffusion of water within the peptide.

J. A. Dani and D. G Levitt [6] explained the importance of water mobility on protein surfaces and provided insights into the behavior of water and ions in the gramicidin channel. M. Engels *et. al*. [7] performed a diffusion reaction within 0.76 ns molecular dynamics simulation on a self-assembled peptide nanotube in water. D. S. Banks and C. Fradin [8] investigated protein diffusion in highly concentrated solutions mimicking cellular environments. J. A. Dix and A. S. Verkman [9] examined the impact of molecular crowding on solute diffusion in solution, cellular aqueous compartments, and membranes. H. Liu *et. al.* [10] synthesized and tested the cyclic peptide nanotubes

(CPNs) for drug delivery, specifically using (Trp-d-Leu)4-Gln-d-Leu CPNs to transport the antitumor drug 5-fluorouracil (5-FU). X. Zhao and H. Jin [11] obsereved the hydrogen diffusion in supercritical water, specifically in the context of supercritical water gasification of coal for hydrogen production. R. P. Koirala *et. al.* [12] studied the molecular dynamics (MD) simulations of glucose in water at different temperature (298.15 K, 303.15 K, 308.15 K, and 312.15 K) to find the transport and structural properties. The self-diffusion coefficients of glucose and water have been estimated from mean square displacement plot (MSD) by using Einstein's relation.

From the above studies, we are motivated to study the structural and dynamical behavior, as well as the diffusion of water in amphiphilic α–helix peptide at different temperatures. This study will seek to shed light on the intricate dynamics that drive peptide functionality, leading to valuable insights that can revolutionize drug development, biomaterial design, and therapeutic interventions, ultimately shaping the future of biomedical research and innovation.

Fig. 1: Molecular structure of hydrophilic amphiphatic helical peptide in 3D representation.

Out of the various peptides, we are motivated to work on alpha-helix types of peptide which is found in an α-helical structure at which the amino acid residues are distributed in the secondary structural form of opposite polar (hydrophilic) and nonpolar (hydrophobic) faces [13, 14, 15, 16]. The physical and biological properties of different peptides that interact with lipid or membrane surfaces have been postulated to be influenced by amphiphilic helical configurations [17, 18, 19, 20]. A typical 3D structure of hydrophilic amphipathic helical peptide is shown in Fig. 1. Similarly, the cpk representation of hydrophilic amphipathic helical peptide is depicted in Fig. 2, where blue, green, red, and white represent nitrogen, carbon, oxygen, and hydrogen atoms, respectively. Nowadays, a large number of therapeutic and diagnostic peptides have been approved and are available, and many are the subjects of clinical trials or in the later stages, which suggests that peptides have secured a future in medicine and diagnosis. Many therapeutic peptides are used to manage a large number of diseases ranging from cancer, cardiovascular, metabolic disorders, infectious diseases, and so on. It might also be helpful in preventing the formation of cataracts in the eyes [21]. A significant amount of research is being undertaken to emphasize peptide based inhibitors for disease management. Thus, we expect that emerging peptide technologies will broaden therapeutic applications, which also motivate us to go more insight into the peptides to explore the diffusion related properties.

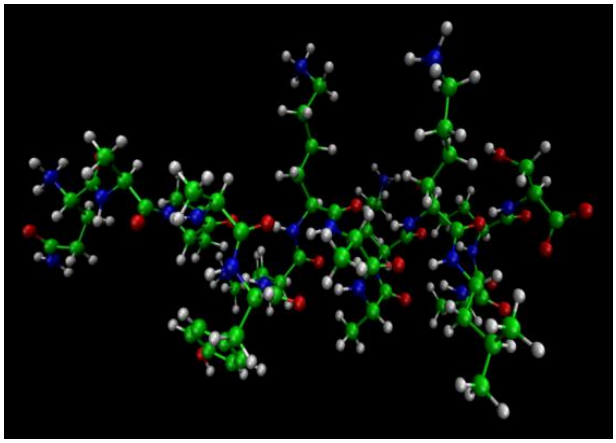

Fig. 2: Molecular structure of hydrophilic amphiphatic helical peptide in cpk representation.

THEORETICAL MODEL AND COMPUTATIONAL DETAILS

Molecular dynamics (MD) is the method of simulation used to study the physical movements of atoms and molecules. In MD simulation, the position and velocities of the particle evolve by the laws of classical mechanics and Newton's equation of motion given as [22, 23]:

$$m_i \frac{\partial^2 r_i}{\partial t^2} = \mathrm{F}_i(r_i) = -\nabla U_i(r_i) \quad \text{.....(1)}$$

Where, i = 1, 2, 3,.....N is no. of atoms, m_i is the mass of i^{th} atom, r_i is the position vector of i^{th} atom. The negative gradient of the potential (U_i) on the right hand side is equal to the force F_i acting on the i^{th} atom with mass m_i. All the parameters required to deal potentials are calculated based on the system selected and chosen environment. The short descriptions of

diffusion theory and computational details are explained in the following sections.

THEORY OF DIFFUSION

Diffusion is the random movement of substances from a higher concentration zone to a lower concentration zone, giving birth to molecular diffusion [24] and is essential for various biological processes [25]. Diffusion moves freely in liquid and gases. In living organisms, useful molecules enter the body cells and waste products are removed by the diffusion process. The rate of diffusion is affected by various factors like temperature, the viscosity of the fluid, area of interactions, size of the particles and concentration gradient [26]. Normally, diffusion is categorized into self-diffusion and binary (mutual) diffusion. The diffusion coefficient is governed by Fick's law of diffusion. According to Fick's law, particle flux is proportional to the concentration gradient [9, 27, 28] which is given by,

$$J = -D\nabla C(r,t) \qquad (2)$$

Where, C(r,t) is the concentration of diffusing substance which is function of position r and time t ; and D is the diffusion coefficient whose dimensions is $\text{length}^2\text{time}^{-1}$. The negative sign indicates that the diffusion occurs in the direction opposite to that of increasing concentration. As an extension of Fick's law, Einstein provided the relationship between diffusion coefficient and mean squared displacement over time. The Einstein's relation [29] for diffusion is provided by,

$$D = \lim_{t\to\infty} \frac{\langle |r(t)-r(0)|^2\rangle}{2dt} \qquad (3)$$

Where, d is degree of dimensions, t is the time, and $\langle |r(t) - r(0)|^2\rangle$ is the mean square displacement (MSD) at time t.

COMPUTATIONAL DETAILS

System setup and Molecular Dynamics Simulations

In order to model peptide, a PDB ID 1djf.pdb was taken from the protein data bank (pdb), an authorized pdb website (www.rcsb.org). The molecule was in complete form as requirement of present study, so no modification was done in the original structure. The topology and parameters for the system setup and molecular dynamics (MD) simulations were taken from CHARMM-GUI [30, 31]. The molecule was solvated into a cubical box of dimension 5×5×5 nm^3 with TIP3P water model and the solvation box was neutralized by adding 10 potassium and 13 chloride ions using add ions feature from the same force field systematically [30, 31]. The ions are added in peptide molecular dynamics simulations to neutralize the overall charge, mimic physiological environments, modulate electrostatic interactions, maintain proper solvation effects, simulate realistic salt concentrations and ionic strengths, within the frame which maintains criteria of periodic boundary conditions. After preparing all the components individually, we merged each of them accordingly to make the system.

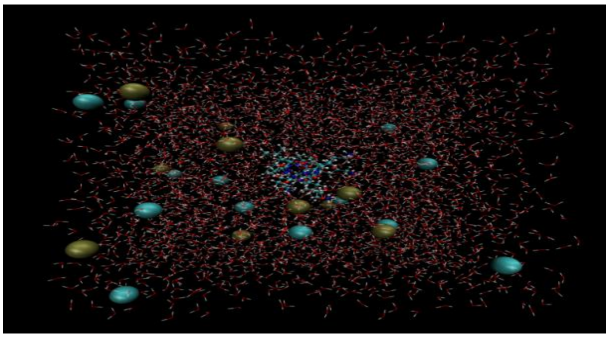

Fig. 3: System ready to be simulated.

Fig. 3 represents complete system under the study ready for the simulation. The system consists of a total of 11517 atoms: 3752 water molecules (11256 atoms), 238 atoms in protein form, 10 potassium, and 13 chloride ions. The system mimics as an aqueous solution of KCl_2 having concentration 0.15 gm/cc. We have used the latest and updated version of the CHARMM force field, that is CHARMM36 all-atom additive force field. For the model, we used separate CHARMM36 all-atom additive force field parameters for proteins [32, 33], nucleic acids [34], hydrogen lipids [35], water and ions [36] to make perfect topology of system. To cope with the desired qualities, three fundamental procedures were used: energy minimization, system equilibration, and production run. The entire simulations were carried out at temperatures 290 K, 300 K, and 310 K using the steepest-descent algorithm. We subjected the system to the process of energy minimization for 50000 steps. Constant temperature control is carried out using a Langevin thermostat. Long-range Coulomb interactions and full electrostatics interactions of the system are handled by PME (Particle Mesh Ewald) method which is preferable in the simulations with periodic

boundaries. Following the energy minimization, we performed NVT equilibration of 5000000 steps with time step of 2 fs (10 ns) for each temperature. After successful minimization and equilibration, the system is ready for production run which finally produced required parameters used for analysis. For this, we ran a 10 ns with a time step of 2 fs equilibrium production simulation for each temperature.

RESULTS AND DISCUSSION

Energy minimization and equilibration

It is crucial to minimize the energy of system before beginning any simulations or calculations. It determines the proper molecular arrangement in space since the initial system may contain bad contacts, overlapping van der Waals radii. In such cases, the system is out of equilibrium, hence equilibration may not be conserved and MD simulations may fail. In the present calculation, the potential energy curve attains minimum and almost constant value over the time steps after 15000-16000 energy steps. The compact or stable systems attains -50006.30 Kcal(mol)$^{-1}$ of energy indicates the system is converged with minimum energy. The plot of the potential energy of the system as a function of the time step at 300 K is shown in the Fig. 4. Now, system is ready for the equilibration run which actually provides system under thermal equilibrium. Fig. 5 shows how the temperature is distributed to the system throughout 10 ns equilibration at 300 K.

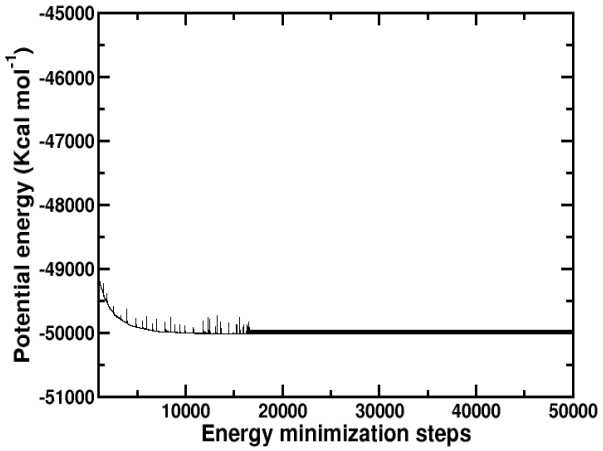

Fig. 4: Energy minimization.

Furthermore, the temperature distribution to the system throughout 10 ns is shown in Table 1. The main aim of present study is diffusion with respect to temperature variation. We here observed equilibrations of the system for temperatures below and above room temperature (290 K and 310K) and compare with room temperature (300K). The nature of energy minimization and equilibation for different systems are resembling. So, figure contains the results of 300K only. However, other results are depicted in the respective table. The symmetrical fluctuation of temperatures and their average confirm the system is in thermal equilibrium at given temperatures. Same kinds of nature is observed in RMSD plot during equilibration (Fig. 6). The average RMSD value was found 0.25 Å for each temperature which also confirms the structure is stable in all three simulations [31]. After minimization and equilibration, we performed a 10 ns simulation and estimated energy profiles, the structure of the system, MSD and diffusion coefficient at each case explained in the respective sections.

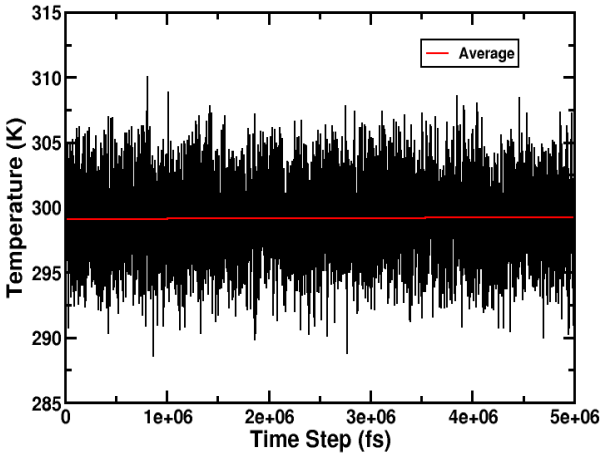

Fig. 5: Temperature fluctuation at 300 K during equilibration.

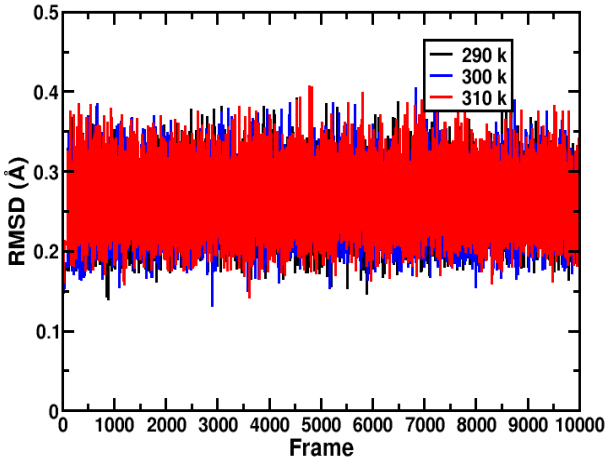

Fig. 6: RMSD at different temperatures.

Table 1: Distribution of temperature during equilibration.

Coupling Temperature (K)	Equilibrium Temperature (K)
290	289.34 ± 0.05
300	299.07 ± 0.06
310	309.12 ± 0.06

Energy profile

Evaluation of different types of energies in MD simulation illustrates how different types of interactions took place among atoms and molecules inside the system. The total energy of the system is contributed by kinetic and potential energy which is the pairwise sum of potential due to bonded and non-bonded interactions. Bonded interactions include bond stretching potential, bond bending potential, and potential due to dihedral interactions. Non-bonded interactions incorporate Lennard Jones and Coulomb interactions. Here, we evaluate the different types of energies possessed by the system at different temperatures during the equilibrium production run. Fig. 7 shows the plot of bond stretching energy, angle vibration energy, dihedral term, improper term, Van der Waals interaction energy, kinetic energy, potential energy, and total energy of the system during equilibrium simulation at 300K and comparative values for different temperatures are depicted in Table 2. The negligible value of the dihedral, and the improper term confirms that the system becomes stable as expected by maximizing energies. From the energy profile, we observed that bond, angle, van der Waal, and KE are all positive energy terms whereas PE and total energies are always negative. While compairing different temperatures, bond stretching has the least contribution to the total energy. The angle vibration has a slightly high positive value than bond stretching. The Van der Waals interactions have significantly more contribution to the total energy than bond stretching. KE has the highest value among the positive energies. The temperature dependency of different energies except VDW interaction energy is increasing linearly with temperature (Table 2 and Table 3). It is perfectly opposite in the case of van der Waals interaction energy, which is slightly decreasing on increasing temperature.

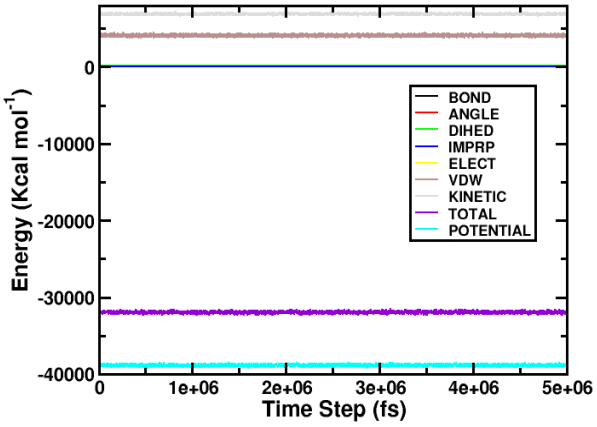

Fig. 7: Plot of different energies at 300 K.

Table 2: Different energies possessed by the system at different temperatures.

Energy Term (Kcal mol^{-1})	Temperatures		
	290 K	300 K	310 K
Bond	41.95 ± 0.11	42.86 ± 0.11	44.01 ± 0.11
Angle	135.75 ± 0.18	138.96 ± 0.18	141.71 ± 0.19
VDW	4204.15 ± 0.18	4090.72 ± 0.18	3983.04 ± 0.19
KE	6661.04 ± 0.12	6885.69 ± 0.12	7116.45 ± 0.13
PE	−39325.04 ± 0.0.18	−38847.05 ± 0.19	−38368.23 ± 0.19
Total	−32664.00 ± 0.22	−31961.35 ± 0.22	−31251.79 ± 0.23

Table 3: Temperature dependency of K.E.

Temperature (K)	KE (Kcal mol^{-1})	KE/T (Kcal mol^{-1})
290	6661.04	22.97
300	6885.69	22.95
310	7116.45	22.96

Radial distribution function

The radial distribution function (RDF) is used to analyze the structural properties of the system. It gives the information about how atoms or molecules are distributed around the reference atom or molecule. Moreover, it gives the idea about the density and probability of atoms or molecules at the

desired distance from the reference atoms or molecules. Here, we computed and analyzed the RDF of different atoms from different reference atoms at different temperatures. The main goal of calculating the RDF of water is to find out the structural property of water under the influence of different temperatures. The RDF plot of peptide-water atoms of TIP3P water throughout the system is given in Fig. 8.

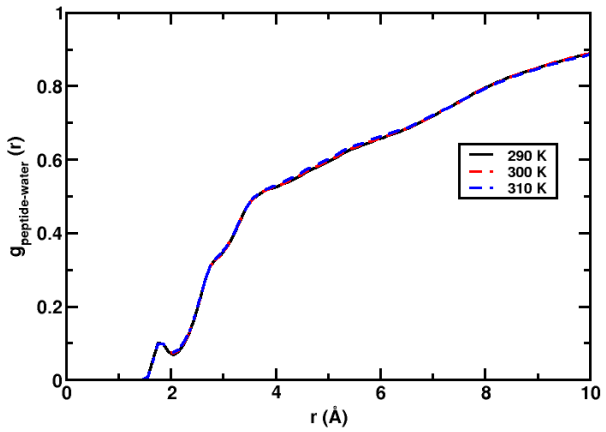

Fig. 8: RDF plot of peptide-water at different temperatures.

The position of the first peak is around 1.8 Å and the second less significant around 3.7 Å for all temperatures. The result is in good agreement with the previous results [38, 39, 40]. The RDF plot of peptide-peptide molecules of water at different temperatures is shown in Fig. 9.

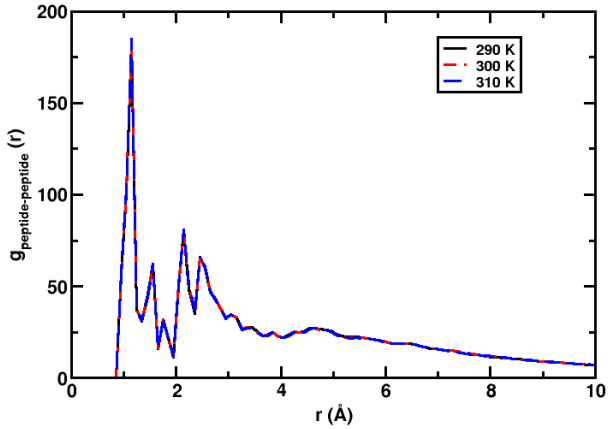

Fig. 9: RDF plot of peptide-peptide at different temperatures.

The position of the first peak is around 1.2 Å for all three temperatures. This result is also in close agreement with previous investigations [7, 39, 40].

The temperature variation of RDF of oxygen-oxygen atoms of water is given in Fig. 10. The first peaks in the graphs represent the positions of the closest neighbors within the first shell. The absence of particles up to the second peak locations is indicated by the troughs. Similarly, the second peaks denote the position of the second closest neighbors, as determined by the following shell, and so on. After a few oscillations, RDF reaches unity and remains reasonably stable up to infinity. This suggests that the molecules are not associated across extended distances which are consistent with other liquid molecule's known properties [41]. Moreover, the height of the first peak is decreasing with an increase in temperature indicating lesser water density at the higher temperature.

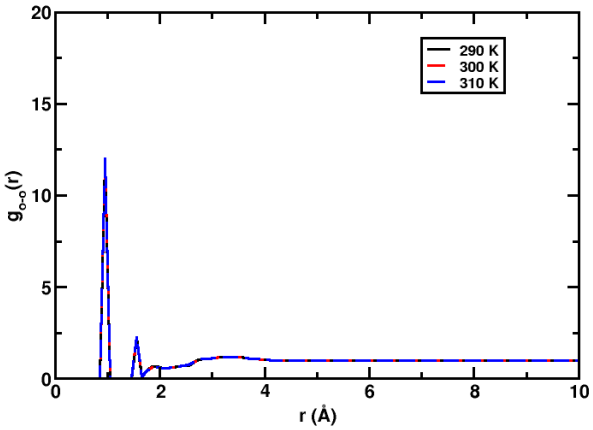

Fig. 10: RDF plot of oxygen-oxygen at different temperatures.

MSD and Diffusion Coefficient

To understand the dynamical behavior of water, we computed the mean square displacement (MSD) and self-diffusion coefficient by using diffusion coefficient tool in VMD [37]. The Self-diffusion coefficient of water at three different temperatures; 290 K, 300 K, and 310 K, respectively were analyzed using the Einstein's relation. The MSD plot of water at different temperatures is shown in Fig. 11. We have carried out 10 ns MD simulation for each temperature. However, the linear relationship has to be required to draw the values of slope in MSD versus time graph. For that, we have selected 100 ps simulation run in the beginning to get the better statistics. The self-diffusion coefficients of water at different temperatures 290 K, 300 K, and 310 K are 0.44×10^{-5} cm^2s^{-1}, 0.48×10^{-5} cm^2s^{-1}, and $0.50\times10^{-5}cm^2s^{-1}$, respectively (Table 4). The self-diffusion coefficient of water was found good agreement with previously reported

values [7]. The result is also valid with the experimental result of self-diffusion coefficient of water [6, 43, 44]. It is seen that when smaller solute molecules are present, water diffuses quicker at a given temperature and hence the MSD curve is steeper [45]. This shows that the MSD of water throughout the system is increasing on increasing temperature. It is because the increase in temperature enhances the kinetic energy and collision frequency of molecules, reducing viscosity, and thereby increasing the diffusion coefficient.

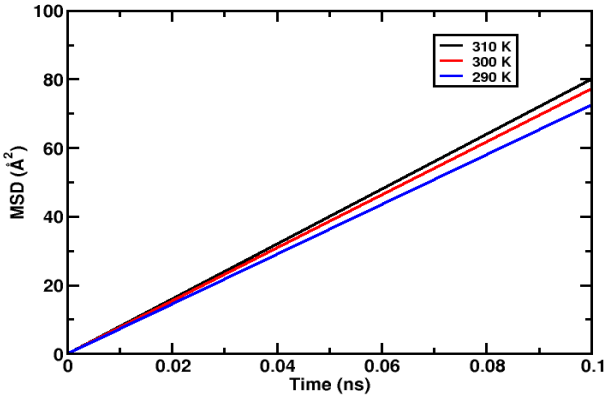

Fig. 11: MSD plot of water at different temperatures.

Table 4: Diffusion coefficient of water at different temperatures.

Temperature (K)	Self-diffusion Coefficient ($\times 10^{-5} cm^2 s^{-1}$)
290	0.44 ± 0.05
300	0.48 ± 0.05
310	0.50 ± 0.05

CONCLUSION

The MD simulation of peptide in water was carried out with a system containing 11517 atoms including 3752 water molecules for various temperatures 290 K, 300 K, and 310 K. We used TIP3P water model for MD simulation. Here, peptide acts as a solute and water as a solvent. The system's energy profile was examined in order to determine the system's equilibrium nature. We calculated and studied the contribution of different energies possessed by the system at equilibrium simulation to the total energy of the system. We discovered that the KE of the system is proportional to the temperature. Furthermore, the average RMSD value was found 0.25 Å which confirms the structure is stable in all three temperatures. The structural properties of both peptide and water in equilibrium were investigated by calculating corresponding radial distribution function (RDF) of peptide-peptide, peptide-water, and water-water. The first peak placements in all RDF plots have changed somewhat as the temperature climbed. Moreover, the heights of the first peak have fallen and their width has expanded. These observations point to an increase in random motion as temperature rises.

Furthermore, at higher temperatures, a wide RDF means more space between molecules. As a result, the molecules are able to travel more freely that increase the diffusion coefficient. We also calculated the self-diffusion coefficient of water. It is clearly seen that the diffusion coefficients as increases as in the order of $D_{310K} > D_{300K} > D_{290K}$. This shows that the MSD of water throughout the system is increasing on increasing temperature . In short, MD simulation approach provides the better result regarding structural and dynamical behavior of peptide in water.

Besides of above investigation, peptides play an important role in living cells. It is recommended to insightful study on structural and dynamic behaviors to know about the anomalous diffusion and other related properties inside the cells. It also has broad applications in the field of medicines. Further research and developments have to be encouraged to harness the potential application of peptides in therapeutic and diagnostic advancements. The peptide based technologies for peptide drug design and optimization is in the progress which is really a challenging task but interesting to research community.

REFERENCES

[1] Schoneberg, J.; & Noe, F. ReaDDy-a software for particle-based reaction-diffusion dynamics in crowded cellular environments. *PloS One*, **8** (9): e74261 (2013).

[2] Chakrabarti, S.; Guha, S.; & Majumder, K. Food-derived bioactive peptides in human health: Challenges and opportunities. *Nutrients*, **10** (11): 1738 (2018).

[3] Deb, P. K.; Al-Attraqchi, O.; Chandrasekaran, B.; Paradkar, A.; & Tekade, R. K. Protein/peptide drug delivery systems: practical considerations in pharmaceutical product development. *In Basic Fundamentals of Drug Delivery*, 651-684 (2019).

[4] Su, M.; Ling, Y.; Yu, J.; Wu, J.; & Xiao, J. Small proteins: untapped area of potential biological importance. *Frontiers in Genetics*, **4**: 286 (2013).

[5] Smith, S.; Cianci, C.; & Grima, R. Macromolecular crowding directs the motion of small molecules inside cells. *Journal of the Royal Society Interface*, **14** (131): 20170047 (2017).

[6] Dani, J. A.; & Levitt, D. G. Water transport and ion-water interaction in the gramicidin channel. *Biophysical Journal*, **35** (2): 501-508 (1981).

[7] Engels, M.; Bashford, D.; & Ghadiri, M. R. Structure and dynamics of self-assembling peptide nanotubes and the channel-mediated water organization and self-diffusion: A molecular dynamics study. *Journal of the American Chemical Society*, **117** (36): 9151-9158 (1995).

[8] Banks, D. S., & Fradin, C. Anomalous diffusion of proteins due to molecular crowding. *Biophysical journal*, **89** (5): 2960-2971 (2005).

[9] Dix, J. A., & Verkman, A. S. Crowding effects on diffusion in solutions and cells. *Annual Review of Biophyics*, **37**: 247-263 (2008).

[10] Liu, H., Chen, J., Shen, Q., Fu, W., & Wu, W. Molecular insights on the cyclic peptide nanotube-mediated transportation of antitumor drug 5-fluorouracil. *Molecular Pharmaceutics*, **7** (6): 1985-1994 (2010).

[11] Zhao, X., & Jin, H. Investigation of hydrogen diffusion in supercritical water: A molecular dynamics simulation study. *International Journal of Heat and Mass Transfer*, **133**: 718-728 (2019).

[12] Koirala, R. P., Dawanse, S., & Pantha, N. Diffusion of glucose in water: A molecular dynamics study. *Journal of Molecular Liquids*, ***345*:** 117826 (2022).

[13] Kitamura, A.; Kiyota, T.; Tomohiro, M.; Umeda, A.; Lee, S.; Inoue, T.; & Sugihara, G. Morphological behavior of acidic and neutral liposomes induced by basic amphiphilic α-helical peptides with systematically varied hydrophobic-hydrophilic balance. *Biophysical Journal*, **76** (3): 1457-1468 (1999).

[14] Gulsevin, A.; & Meiler, J. Prediction of amphipathic helix-membrane interactions with Rosetta. *PLoS Computational Biology*, **17** (3): e1008818 (2021).

[15] Kaiser, E. T.; & Kezdy, F. J. Secondary structures of proteins and peptides in amphiphilic environments.(A review). *Proceedings of the National Academy of Sciences*, **80** (4): 1137-1143 (1983).

[16] Blanc, J. P.; Taylor, J. W.; Miller, R. J.; & Kaiser, E. T. Examination of the requirement for an amphiphilic helical structure in beta-endorphin through the design, synthesis, and study of model peptides. *Journal of Biological Chemistry*, **258** (13): 8277-8284 (1983).

[17] Segrest, J. P.; Jackson, R. L.; Morrisett, J. D.; & Gotto Jr, A. M. A molecular theory of lipid protein interactions in the plasma lipoproteins. *FEBS Letters*, **38** (3): 247-253 (1974).

[18] Edelstein, C.; Kezdy, F. J.; Scanu, A. M.; & Shen, B. W. Apolipoproteins and the structural organization of plasma lipoproteins: human plasma high density lipoprotein-3. *Journal of Lipid Research*, **20** (2): 143-153 (1979).

[19] DeGrado, W. F.; Kezdy, F. J.; & Kaiser, E. T. Design, synthesis, and characterization of a cytotoxic peptide with melittin-like activity. *Journal of the American Chemical Society*, **103** (3): 679-681 (1981).

[20] Kroon, D. J.; Kupferberg, J. P.; Kaiser, E. T.; & Kezdy, F. J. Mechanism of lipid-protein interaction in lipoproteins. A synthetic peptide-lecithin vesicle model. *Journal of the American Chemical Society*, **100** (18): 5975-5977 (1978).

[21] Baig, M. H.; Ahmad, K.; Saeed, M.; Alharbi, A. M.; Barreto, G. E.; Ashraf, G. M.; & Choi, I. Peptide based therapeutics and their use for the treatment of neurodegenerative and other diseases. *Biomedicine & Pharmacotherapy*, **103**: 574-581 (2018).

[22] Phillips, J. C. *et. al.* Scalable molecular dynamics with NAMD. *Journal of Computational Chemistry*, **26** (16): 1781-1802 (2005).

[23] Andoh, C. N.; & Banini, G. K. Molecular dynamics simulation of mechanical deformation of austenitic stainless steels (Fe-Ni-Cr alloys) at supercritical water conditions. *Journal of Applied Science & Technology*, **22**: (2017).

[24] Schavemaker, P. E.; Boersma, A. J.; & Poolman, B. How important is protein diffusion in prokaryotes. *Frontiers in Molecular Biosciences*, **5**: 93 (2018).

[25] Brangwynne, C. P.; Koenderink, G. H.; MacKintosh, F. C.; & Weitz, D. A. Cytoplasmic diffusion: molecular motors mix it up. *The Journal of Cell Biology*, **183** (4): 583-587 (2008).

[26] De Kee, D.; Liu, Q.; & Hinestroza, J. Viscoelastic (non-Fickian) diffusion. *The Canadian Journal of Chemical Engineering*, **83** (6): 913-929 (2005).

[27] Mehrer, H.; & Stolwijk, N. A. *Heroes and highlights in the history of diffusion*, (2009).

[28] Frenkel, D.; Smit, B.; & Ratner, M. A. *Understanding molecular simulation: from algorithms to applications*, **2**: San Diego: Academic press (1996).

[29] Malenkov, G. Liquid water and ices: understanding the structure and physical properties. *Journal of Physics: Condensed Matter*, **21** (28): 283101 (2009).

[30] Lee, J.; Cheng, X.; Swails, J. M.; Yeom, M. S.; Eastman, P. K.; Lemkul, J. A.; & Im, W.

CHARMM-GUI input generator for NAMD, GROMACS, AMBER, OpenMM, and CHARMM/OpenMM simulations using the CHARMM36 additive force field. *Journal of Chemical Theory and Computation*, **12** (1): 405-413 (2016).

[31] Jo, S.; Kim, T.; Iyer, V. G.; & Im, W. CHARMM-GUI: a web□based graphical user interface for CHARMM. *Journal of Computational Chemistry*, **29** (11): 1859-1865 (2008).

[32] MacKerell Jr, A. D.; Feig, M.; & Brooks, C. L. Improved treatment of the protein backbone in empirical force fields. *Journal of the American Chemical Society*, **126**: 698–699 (2004).

[33] MacKerell Jr, A. D.; Bashford, D.; Bellott, M. L. D. R.; Dunbrack Jr, R. L.; Evanseck, J. D.; Field, M. J., & Karplus, M. All-atom empirical potential for molecular modeling and dynamics studies of proteins. *The Journal of Physical Chemistry B*, **102** (18): 3586-3616 (1998).

[34] Hart, K.; Foloppe, N.; Baker, C. M.; Denning, E. J.; Nilsson, L.; & MacKerell Jr, A. D. Optimization of the CHARMM additive force field for DNA: Improved treatment of the BI/BII conformational equilibrium. *Journal of Chemical Theory and Computation*, **8**(1): 348-362 (2012).

[35] Klauda, J. B.; Venable, R. M.; Freites, J. A.; O'Connor, J. W.; Tobias, D. J.; Mondragon-Ramirez, C.; & Pastor, R. W. Update of the CHARMM all-atom additive force field for lipids: validation on six lipid types. *The Journal of Physical Chemistry B*, **114** (23): 7830-7843 (2010).

[36] Beglov, D.; & Roux, B. Finite representation of an infinite bulk system: solvent boundary potential for computer simulations. *The Journal of Chemical Physics*, **100** (12): 9050-9063 (1994).

[37] Nutt, D. R.; & Smith, J. C. Molecular dynamics simulations of proteins: Can the explicit water model be varied. *Journal of Chemical Theory and Computation*, **3** (4): 1550-1560 (2007).

[38] Jain, S. S.; Suresh, A.; & Pirogova, E. Effects of oscillating electric fields on conotoxin peptide conformation: A molecular dynamic simulation study. *Journal of Molecular Graphics and Modelling*, **103**: 107799 (2021).

[39] Maity, A.; Choudhury, A. R.; & Chakrabarti, R. Effect of Stapling on the Thermodynamics of Protein-Peptide Binding. *bioRxiv*, 2020-12 (2020).

[40] Turner, M.; Mutter, S. T.; Kennedy-Britten, O. D.; & Platts, J. A. Molecular dynamics simulation of aluminium binding to amyloid-β and its effect on peptide structure. *PLoS One*, **14** (6): e0217992 (2019).

[41] Pokharel, S.; Pantha, N.; & Adhikari, N. P. Diffusion coefficients of nitric oxide in water: A molecular dynamics study. *International Journal of Modern Physics B*, **30** (27): 1650205 (2016).

[42] Giorgino, T. Computing diffusion coefficients in macromolecular simulations: the Diffusion Coefficient Tool for VMD. *Journal of Open Source Software*, **4** (41): 1698 (2019).

[43] Chiu, S. W.; Jakobsson, E.; Subramaniam, S.; & McCammon, J. A. Time-correlation analysis of simulated water motion in flexible and rigid gramicidin channels. *Biophysical Journal*, **60** (1): 273-285 (1991).

[44] Chiu, S. W.; Subramaniam, S.; & Jakobsson, E. Simulation study of a gramicidin/lipid bilayer system in excess water and lipid. I. Structure of the molecular complex. *Biophysical Journal*, **76** (4): 1929-1938 (1999).

[45] Khanal, S. P.; Kandel, Y. P.; & Adhikari, N. P. Transport properties of zwitterion glycine, diglycine, and triglycine in water. *AIP Advances*, **9** (6): 065303 (2019).